2D And 3D Numerical Simulation The Discontinuous Wave on Group of Structures

Le Thi Thu Hien, Quang Hung Nguyen

***Abstract*: The aim of this paper is to investigate the capability of the 2D and 3D numerical models to simulate the flow of flood waves in the presence of several structures on downstream. The 2D numerical model based on Finite Volume method (FVM)-Godunov type to solve 2D non shallow water equations is proposed. The commercially-available CFD software package Flow 3D solved Navier-Stokes equations along the volume of fluid (VOF) method to track the location of the free surface at the air water interface. The computed results such as the stage hydrographs, the variation of velocity components with respect to time were compared to the results of the experiments and showing good agreement. In addition, force acting on each structure is computed and verified with the experimental data.**

Keywords: Flood wave; 2D numerical model; Flow 3D; group of structures; force.

I. INTRODUCTION

Dam failure often causes huge damage on human and facility in downstream valley. [1] The study of the influence of dam break flow on structure or group of structure plays important role on giving some early warnings or increasing level of safety awareness at downstream region. Mathematical model is always considered as an effective tool in predicting propagation of flood wave with difference scenarios. Recently, Computational Fluid Dynamic (CFD) simulation becomes wide-spread for solving problems involving fluid flow. 2D mathematical model based on shallow water equations (SWE) has been using widely in simulating hydraulic characteristics.[2-6]. Much attention was paid to the hydrodynamic parameters such as: water depth, velocity profile of discontinuous flow such as Aureli et al, [7]; Soares-Frazao and Yves Zech, [8]. Although, there are few studies concerning about the force due to impact of the flash flood on structure or group of building by both physical and numerical models. Aureli et al, [7] used experimental tests and 2D and 3D numerical models to evaluate force due to the impact of a dam break wave on a structure, meanwhile, Shige-eda and J. Akiyama [9] selected a physical method and 2D numerical scheme to determine the influence of dam break wave on group of square pillars. However, SWE does not account for turbulent term, thus, if the flow involves the interaction of fluid and solid such as the water flow around group of building, the SWE may not simulate accurately this hydraulic character. Recently, 3D numerical model has been developing quickly in solving many complicated problems related to fluid motion.[10-11]. Therefore, in this research, test case of rapid flow over group of obstacles presented in the aforementioned paper is reproduced by both the proposed 2D numerical scheme and a 3D mathematical model. A commercial available CFD model, which solves the Reynolds averaged Navier-Stokes (RANs) equations Flow 3D is utilized. Besides, 2D numerical model based on finite volume method (FVM) and MUSCL (Monotonic Upwind Scheme for Conservation Laws) procedure is also applied to obtain second order accuracy in space and time when solving SWEs. Several hydraulic characteristics are estimated such as: flooding map, water depth and velocity hydrographs. Especially, force due to dam break flow exerting to different obstacles is also simulated.

Revised Manuscript Received on June 12, 2019.

Le Thi Thu Hien, Thuyloi University, 175 Tay Son , Dong Da, Hanoi, Vietnam.

Quang Hung Nguyen, Thuyloi University, 175 Tay Son , Dong Da, Hanoi, Vietnam.

II. BASIS OF SCIENCE AND METHODOLOGY

A. *2D numerical model*

1) Governing 2D mathematical model

If the turbulent viscous terms is neglected, derive Navier-Stokes equations in depth-integrating and assume pressure is hydrostatic, two-dimensional non-linear shallow water equations (2D-NSWE) can be written in the conservation form:

$$\frac{\partial \mathbf{U}}{\partial t}+\frac{\partial \mathbf{G}(\mathbf{K})}{\partial x}+\frac{\partial \mathbf{H}(\mathbf{K})}{\partial y}=\mathbf{S}(\mathbf{K}) \quad (1)$$

where: $\mathbf{K}=\begin{bmatrix} h \\ hu \\ hv \end{bmatrix}$; $\mathbf{G}(\mathbf{K})=\begin{bmatrix} hu \\ hu^2+0.5gh^2 \\ huv \end{bmatrix}$;

$$\mathbf{H}(\mathbf{K})=\begin{bmatrix} hv \\ huv \\ hv^2+0.5gh^2 \end{bmatrix};\mathbf{S}(\mathbf{K})=\begin{bmatrix} 0 \\ gh\left(S_{0x}-S_{fx}\right) \\ gh\left(S_{0y}-S_{fy}\right) \end{bmatrix}$$

$$S_{0x}=-\frac{\partial z_b}{\partial x};\ S_{0y}=-\frac{\partial z_b}{\partial y};$$

$$S_{fx}=\frac{n^2u\sqrt{u^2+v^2}}{h^{4/3}};\ S_{fy}=\frac{n^2v\sqrt{u^2+v^2}}{h^{4/3}}$$

K is the vector of conserved variables; **G** and **H** are flux vectors. S_{0x}, S_{0y}, S_{fx}, S_{fy} are bed slopes and friction slopes along the same directions of source term **S**; n is Manning roughness coefficient; g is gravity acceleration.

x, y are orthogonal space coordinates on a horizontal plane and t is the time; h and z_b are water depth and bottom elevation; u, v are velocity components along x- and y-directions.

In the finite volume framework, on a Cartesian computational domain, applying Godunov type scheme, the flow variables are updated to a new time step by using the following equation:

$$\mathbf{K}_{i,j}^{k+1} = \mathbf{K}_{i,j}^{k} - \frac{\Delta t}{\Delta x}\left[\mathbf{G}_{i+1/2,j} - \mathbf{G}_{i-1/2,j}\right] - \frac{\Delta t}{\Delta y}\left[\mathbf{H}_{i,j+1/2} - \mathbf{H}_{i,j-1/2}\right] + \Delta t\mathbf{S}_{i,j} \quad (2)$$

where k index is time levels; i and j are space indices in x- and y- directions; Δt are time step; Δx and Δy are two cell sizes of the grid cells.

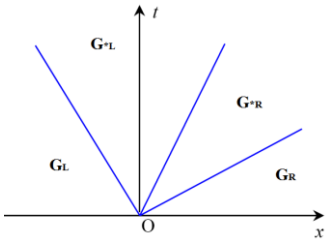

Fig. 1 HLLC solution in x direction of Riemann problem

Interface fluxes $\mathbf{G}_{i\pm1/2,j}$ and $\mathbf{H}_{i,j\pm1/2}$ are approximated by HLLC scheme. For example:

$$\mathbf{G}_{i+1/2} = \begin{cases} \mathbf{G}_L & if \quad s_1 \ge 0, \\ \mathbf{G}_{*L} & if \quad s_1 < 0 \le s_2, \\ \mathbf{G}_{*R} & if \quad s_2 < 0 \le s_3, \\ \mathbf{G}_R & if \quad s_3 \le 0, \end{cases} \quad (3)$$

where, $\mathbf{K}_L$ and $\mathbf{K}_R$ are the variable vectors defined by left and the right states of two adjacent cells of Riemann problem, respectively; $\mathbf{G}_L = \mathbf{G}(\mathbf{K}_L)$ and $\mathbf{G}_R = \mathbf{G}(\mathbf{K}_R)$. $\mathbf{G}_{*L}$ and $\mathbf{G}_{*R}$ are the numerical fluxes in the left and the right sides of the middle region of the Riemann solution which is divided by a contact wave. Flux vector $\mathbf{G}_*$ in the middle region that is evaluated by the following equation:

$$\mathbf{G}_* = \frac{s_3\mathbf{G}(\mathbf{K}_L) - s_1\mathbf{G}(\mathbf{K}_R) + s_1 s_3(\mathbf{K}_R - \mathbf{K}_L)}{s_3 - s_1} \quad (4)$$

where s_1, s_2 and s_3 are estimates of the speeds of the left, contact and right waves, respectively.

$$s_1 = \begin{cases} min(u_L - a_L;\ u_* - a_*) & if \quad h_L > 0, \\ u_R - 2a_R & if \quad h_L = 0, \end{cases}$$

$$s_3 = \begin{cases} max(u_R + a_R;\ u_* + a_*) & if \quad h_R > 0, \\ u_L + 2a_L & if \quad h_R = 0, \end{cases}$$

$$where \quad a_L = \sqrt{gh_L};\ \ a_* = \sqrt{gh_*};\ c_R = \sqrt{gh_R}$$

$$\text{and } s_2 = \frac{s_1 h_R(u_R - s_3) - s_3 h_L(u_L - s_1)}{h_R(u_R - s_3) - h_L(u_L - s_1)} \quad (5)$$

where u_L, u_R, h_L, h_R are the components of velocity and water depth on the left cell and the right cell for a local Riemann problem. h_* and u_* are the Roe average quantities.[12]

Second order accuracy in time and space is achieved by the MUSCL-Hancock procedure with three steps: reconstruction data; evolution of extrapolated values and corrector step, [13]. In this research, slop limiter Minmod technique is used to gain physical results and guarantee the Total Variation Diminishing (TVD) property.

2) Validation the proposed scheme

This test which has analytical solution is very efficient to verify the capability of the present model in dealing with some challenges of numerical modeling such as: bed slope and friction source terms and wet/dry front.

The bottom topography in x direction is defined by: $z_b(x) = \bar{h}(x/\varepsilon)^2$ where $\bar{h}$ and ε are constants.

The analytical solution is firstly carried out by Sampson et al., [14] and later by Song et al., [15], which depends on a bed friction factor τ and hump amplitude ε. Whereas, friction term is defined: $S_f = -\tau \cdot h \cdot u$.

The length of numerical domain is 10000m. For the case with $\tau < p$ where $d = \sqrt{8g\bar{h}/\varepsilon^2}$, the initial conditions of water elevation and velocity are imposed by:

$$\eta(x,0) = \max\left(z_b(x);\ \bar{h} + \frac{\varepsilon^2 M^2 e^{-\pi}}{8g^2\bar{h}}\left(\tau^2/4 - s^2\right) - \frac{M^2 e^{-\pi}}{4g} - \frac{e^{-\pi/2}}{g}(Ms)x\right) \quad (6)$$

$$u(x,0) = 0$$

And the exact solution of the water surface elevation η(x,t) is:

$$\eta(x,t) = e(x,t) - \bar{h}$$

$$e(x,t) = \frac{\varepsilon^2 M^2 e^{-\pi}}{8g^2\bar{h}}\left(-s\tau\sin 2st + \left(\tau^2/4 - s^2\right)\cos 2st\right) - \frac{M^2 e^{-\pi}}{4g} - \frac{e^{-\pi/2}}{g}\left(Ms\cos st + \frac{\tau M}{2}\sin st\right)x \quad (7)$$

where $s = \sqrt{d^2 - \tau^2}/2$. M is constant parameter.

The coefficients in equations (6) and (7) are imposed as: ε = 3000m, $\bar{h}$ = 10m, τ = 0.001s^{-1} and M = 5m/s.

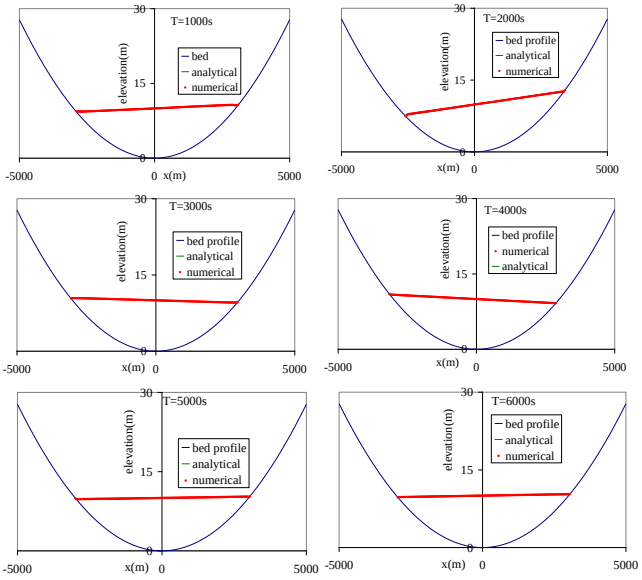

Fig. 2 Water surface elevations at: *t* = 1000*s*, *t*= 2000*s*, *t* = 3000*s*, *t* = 4000*s*, *t*=5000*s*, *t* = 6000*s*.

Computational domain is divided into 400 cells and total time simulation is 6000*s* as in the reserach of Song et al., [15].

Fig. 2 indicates the excellent agreement between simulated water surface elevation and analytical results at difference times. The wet/dry interfaces are correctly reproduced, thus validating the well-balanced wetting and drying algorithm

B. *3D Eulerian*

In this study, a three-dimensional dam-break flow is simulated by using Flow-3D model, a powerful commercial software based on finite volume method (Flow-3D user's manual). One of the main characteristic of turbulent flow is the fluctuation of velocity fields which generate the mixing of transported quantities like momentum and energy. Because of the high frequencies of the fluctuations it is difficult to simulate directly many practical problems due to their high computational cost. Therefore, the time-average equations are used instead of instantaneous equations to avoid the small scales issues and reduce the number of equations. The time-average process can be called Reynolds decomposition. For velocity components: $u_i = \overline{u_i} + u'_i$

Thus the Navier-Stokes equations written with average terms (RANS) can be expressed as:

$$\frac{\partial \overline{u_i}}{\partial x_i} = 0$$

$$\frac{\partial \overline{u_i}}{\partial t} + \overline{u_j}\frac{\partial \overline{u_i}}{\partial xj} = -\frac{1}{p}\frac{\partial \overline{p}}{\partial x_j} + \nu\frac{\partial^2 \overline{u_i}}{\partial x_i \partial x_j} - \frac{\partial \overline{u'_i u'_j}}{\partial xj} + g_i \quad (8)$$

where $\overline{u}$ and $\overline{p}$ are average values of velocity and pressure, respectively. g is gravitational acceleration.The additional term $\overline{u'_i u'_j}$ are called Renolds stress and must be modelled by a turbulent model to solve the equation (8). Renormalization Group (RNG) turbulent model is employed for simulation due to its high accuracy in comparison with other available turbulent model in Flow 3D such as k, k and ε.[16,17]

III. RESULTS AND DISCUSION

An experiment test presented in Shige-eda, [9] is reproduced in this research. Configuration of physical model involves one reservoir with its dimensions (3.0x1.93) m and a flood plain (Fig. 3). They are separated by a dam. Computational domain has horizontal bottom bed. The 0.5m-gate of dam is located far from the left side of 0.75m. This gate can be removed instantaneously. At downstream, three boundaries are opened. Initial water depth in reservoir is 0.2m and downstream is dry. The presence of 10 square pillars was constructed by placing 0.06m wide and 0.2m tall in flood plain. Its coordinates (x_{low}, x_{high}, y_{low}, y_{high}) are: Column A (1.045, 1.105; -0.03, 0.03)m; Column B (1.195, 1.255; -0.3, -0.24)m; Column C (1.045, 1.105; -0.15, -0.09)m; Column D (1.195, 1.255; -0.15, -0.09)m; Column E (1.045, 1.105; -0.30, -0.24)m; Column F (1.195, 1.255; -0.30, -0.24)m. The coordinate of three gauges a, b and c are (0.585;0.00)m, (0.585; -0.5)m and (0.835; -0.75)m, respectively. Observed data was provided such as: water depth profile; two components of velocity in x and y directions observed at three study points. Two component of forces due to fluid flow exert to 6 columns were also collected.

In order to obtain numerical results by 2D mathematical model, computational domain is divided by Catersian mesh with $\Delta x = \Delta y = 0.1$m; Courant number C_r is set equal to 0.9; critical water depth $h_e = 10^{-4}$m is utilized to indicate whether cell is wet or dry. Manning coefficient n is set equal to 0.007.

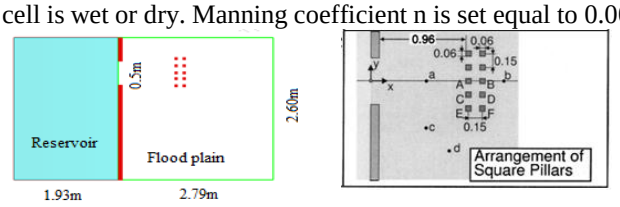

Fig. 3 Experimental configuration

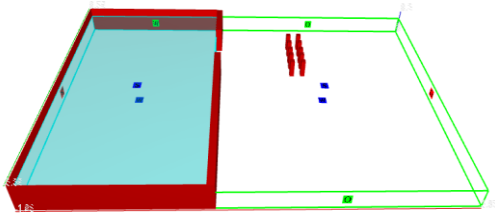

Fig. 4 Computational domain in Flow 3D

To simulate the dam-break flows and their impact to obstacles, the flow region in Flow 3D is subdivided into rectangular cells which each cell has their own local average value of dependent variables. Two mesh blocks are set up: Block 1 is inside reservoir with 3 wall-boundaries. Block 2 is flood plain area where 3 sides of boundary are free out flow. The boundary between two blocks is symmetry.

A. *Flooding maps*

1) 2D numerical scheme

Figure 5 indicates the comparison numerical and physical results of flooding maps at t= 1.25s and t = 1.5s obtained by Shigeeda, [9] with the numerical one of the 2D proposed scheme. A very good matching can be observed between author's work and experimental solution. In both computational time t=1.25s and 1.5s, three "foot toe" of wetting front is quite fit with empirical one, whereas, Shigeeda's computed solution is not.

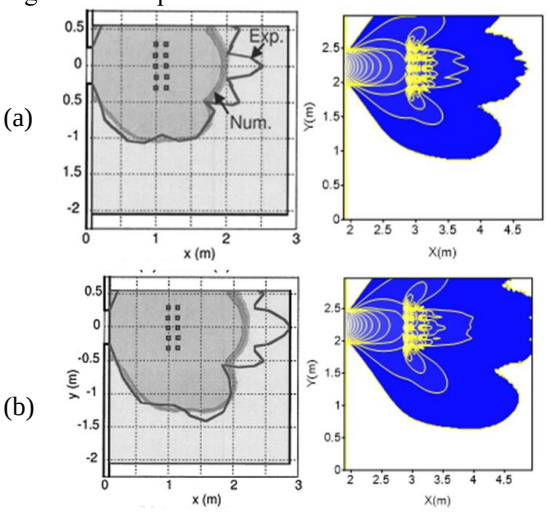

Fig. 5 Inundated maps at t = 1.25s (a) and t = 1.5s (b). Grey color: Shigeeda's result; Blue color: 2D proposed scheme

2) Flow 3D simulation

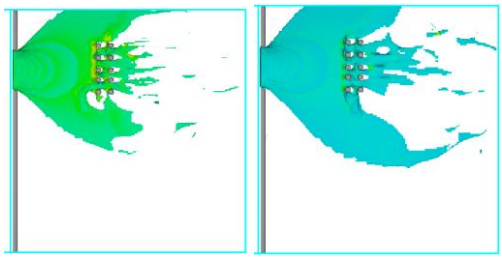

Fig. 6 Flooding maps at t=1.25s (left) and t=1.5s (right) predicted by Flow 3D

The inundated maps obtained by Flow 3D captured at the same time show the discontinuous of wetted area (Fig.6). Although, the inundated area shape is quite close with the previous 2D solution. Because, Flow 3D model accounts for air entrainment while 2D numerical one does not.

B. *Water depth profile.*

Figures 7 and show the observed and numerical time histories of water depth at three gauges a, b and c. It is shown that the flow depth and velocities increases suddenly in the beginning and then continue to reduce gradually. In particular, at point a near the gate, observed water depth vary rapidly immediately due to the operation of gate, whereas numerical result changes less quickly. In general, the discrepancy appears near initial time, after that, very good matching between them can be observed, showing the capability of the proposed scheme in capturing flood wave propagation. 3D computed results of water depth are more fluctuated than 2D model.

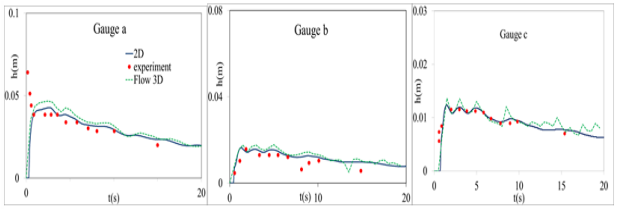

Fig. 7 Water depth profiles at 3 gauges.

C. *Velocity profiles.*

Unfortunately, Flow 3D solution does not give average velocity components so Fig. 8 illustrates only the comparison between 2D numerical and empirical results of two components u and v of velocity following two directions x and y. The larger discrepancy can be seen between two results in comparison with previous solution of water depth. Figure 9 indicates velocity maps at very first time 1.25s and 1.5s. In almost wetted region, average velocity is around 1.5m/s. It is resonable when magnitude of total observed velocity $V = \sqrt{u^2 + v^2}$ showning in Fig 7 at these time is also approximate equal this value.

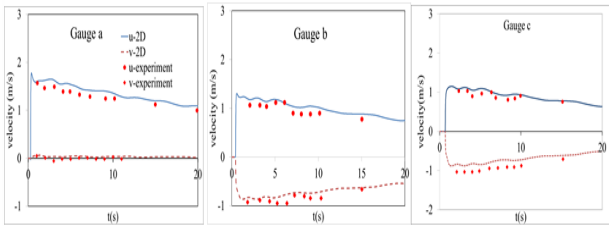

Fig. 8 Velocity component profiles at 3 gauges

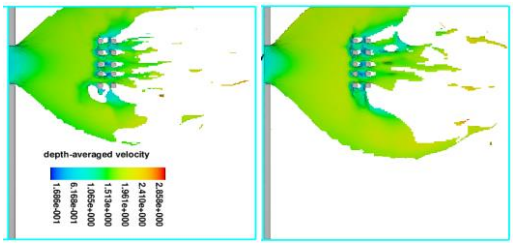

Fig. 9 Velocity magnitude maps at t=1.25s and t=1.5s

D. *Force due to fluid flow acting to structures*

Besides, this work also studies the numerical solution of force acting to 6 square pillars (A, B, C, D, E, F) in x direction. In 2D numerical scheme, component of force F_x in flow direction is calculated by momentum equation in x axis.With hypothesis the pressure is hydrostatic, the net force perpendicular to the vertical wall at each time step is estimated by using momentum equation applied for the control volume taken around obstacle. The total force is calculated for each cell adjacent to the two walls normal to the x-direction. In case the computational mesh is uniform and the solid walls are perpendicular to the x-axis (along the column i at front side and column r at back side), the force at the time level k is computed by:

$$F^k{}_x = \sum_{j_1}^{j_2}\left[\rho g\frac{\left(h_{i,j}^k\right)^2}{2}\Delta y - \rho\frac{\left((uh)_{i,j}^k\right)^2}{h_{i,j}^n}\Delta y\right] - \sum_{j_1}^{j_2}\left[\rho g\frac{\left(h_{r,j}^k\right)^2}{2}\Delta y - \rho\frac{\left((uh)_{r,j}^k\right)^2}{h_{r,j}^k}\Delta y\right] \quad (9)$$

For the Flow-3D software, to estimate the force exerted to a building, the total force in longitudinal (x) direction is considered as a sum of elemental forces calculated in each cell adjacent to the two walls normal to x direction.Fig. 10 compares the computed force versus time curve of dam break flow acting to six structures A-F (Fig.3) with observed data in first 10 seconds of computational time. The arrival times obtained by two CFD methods at 6 columns are quite fit together. However, at square pillars A, B, C and F, the computed results obtained by Flow 3D is matching more closely with empirical ones than 2D numerical solution. Because this model solve includes Navier – Stokes equations with turbulent terms meanwhile 2D-SWEs does not. The overestimation is seen at column D and E in both numerical methods. 3D computed data is higher than observed force meanwhile 2D solution is lower. Therefore, in calculation of force, Flow 3D gives agreement more reasonably with experimental result than 2D numerical scheme. This conclusion is also achieved in the study of the impact of dam break flow acting to one structure, like Aureli et al, [2].

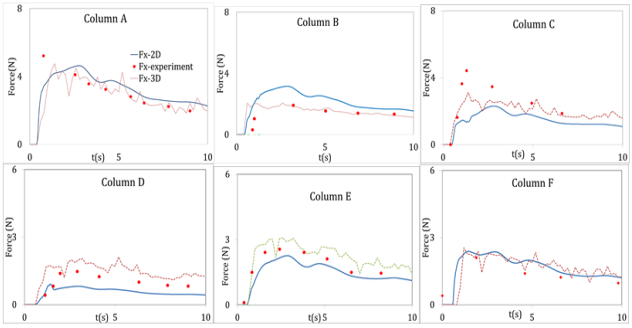

Fig. 10 Comparision of computed and observed forces on structures

IV. CONCLUSION

A numerical scheme based on 2D SWE solved by Finite volume method with MUSCL technique used to obtain second order accuracy in space and time is proposed. This model is applied to reproduce the test case of the flash flow move around group of structures. A 3D commercial software Flow 3D is also utilized to this test. Several numerical results, namely flood extent; water depth, two components of velocity profiles in two direction x and y as well as force due to fluid flow exert to obstacles are estimated. The proposed 2D numerical model evaluates well water depth and velocity profile as well as captures correctly wave propagation. But, Flow 3D gives better estimation of force due to water flow acting to buildings than 2D numerical one.

REFERENCES

1. Pilotti. M; Maranzoni. A; Tomirotti. M and Valerio. G. Gleno Dam Break: Case Study and Numerical Modelling. J. Hydraulic Engineering. 137(4), (ASCE), 480 – 492. (2011)
2. Hou. J; Liang. Q; Simons. F; Hinkelmann. R. A stable 2D unstructured shallow flow model for simulations of wetting and drying over rough terrains. Comput. & Fluids. 82, 132–147. (2013)
3. Hou. J; Liang. Q; Simons. F; Hinkelmann. R. A 2D well balanced shallow flow model for unstructured grids with novel slope source term treatment. Advances in Water Resources. 52, 107 – 131. (2013)
4. Huang. Y; Zhang. N; Pie. Y. Well balanced finite volume scheme for shallow water flooding and drying over arbitrary topography. Engineering Applications of Computational Fluid mechanics. 7(1), 40 – 54. (2013)
5. Valiani. A; Caleffi. V and Zanni. A. Case study: Malpasset Dam-break Simulation using a two dimensional finite volume method. J. Hydraulic Engineering. 128(5) (ASCE), 460- 472. (2002)
6. Yu.E. Shi; R.K. Ray; K.D Nguyen. A projection method based model with the exact C–property for shallow water flows over dry and irregular bottom with using unstructured finite volume technique. Computers and Fluids. 76, 178–195. (2013)
7. Aureli. F, Dazzi. A, Maranzoni. A, Mignosa. P, Vacondio. R. Experimental and numerical evaluation of the force due to the impact of a dam break wave on a structure. Advances in Water Resources, 76, 29-42. (2015)
8. Sandra Soares-Frazao; Yves Zech. Dam-break flow through an idealized city. J. Hydraulic Research, 46(5), 648–65. (2008)
9. Shige-eda. M and Akiyama. J. Numerical and Experimental Study on Two Dimensional Flood Flows with and without Structures, J. Hydraulic Engineering, 129(10), 817-821. (2003)
10. Farzin Salmasi; Aylar Samadi. Experimental and numerical simulation of flow over stepped spillway. Applied Water Science. (2018).
11. Getnet Kebede Demeke, Dereje Hailu Asfaw and Yilma Seleshi Shiferaw. 3D Hydrodynamic Modelling Enhances the Design of Tendaho Dam Spillway, Ethiopia. Water, 11, 82; (2019)
12. Roe. P.L. Approximate Riemann Solvers, parameter vectors and difference schemes. Journal of Computational Physics, 43, 357-372. (1981)
13. Aureli. F, Maranzoni. A, Mignosa. P, Ziveri. C. A weighted surface–depth gradient method for numerical integration of the 2D shallow water equations with topography. Advances in Water Resources, 31, 962-974. (2008)
14. Sampson. J; Easton. A; Singh. M. Moving boundary shallow water flow above bottom topography. ANZIAM (EMAC2005). 47, C373 – C387. (2006)
15. Song. L; Zhou. J; Guo. J; Zou. Q; Liu. Y. A robust well-balanced finite volume model for shallow water flows with wetting and drying over irregular terrain. Advances in Water Resources. 34, 915–932. (2011)
16. Kang. S, Sotiropoulos. F. Numerical modeling of 3D turbulent free surface flow in natural waterways. Advances in Water Resources, 40, 23-36. (2012)
17. Kermani, E.F and Barani, G.A. Numerical simulation of flow over spillway based on CFD method. Scientia Iranica A, 21(1), 91-97. (2014)